Cooperative Regulation of the *Vibrio vulnificus nan* Gene Cluster by NanR Protein, cAMP Receptor Protein, and *N*-Acetylmannosamine 6-Phosphate*[S]

Byoung Sik Kim[‡], Jungwon Hwang[§], Myung Hee Kim[§], and Sang Ho Choi[‡1]

From the [‡]National Research Laboratory of Molecular Microbiology and Toxicology, Department of Agricultural Biotechnology, Center for Food Safety and Toxicology, and Research Institute for Agriculture and Life Sciences, Seoul National University, Seoul 151-921 and the [§]Korea Research Institute of Bioscience and Biotechnology, Daejeon 305-806, South Korea

Background: Catabolic utilization of sialic acid is essential for the pathogenesis of enteropathogens.
Results: NanR, CRP, and ManNAc-6P regulate the *V. vulnificus nan* cluster required for catabolism of Neu5Ac, a sialic acid.
Conclusion: This cooperative regulation leads to precise tuning of the *nan* cluster expression.
Significance: The results shed insight into the understanding of sialate metabolism central to host-microbe interactions.

The *nan* cluster of *Vibrio vulnificus,* a food-borne pathogen, consists of two divergently transcribed operons, *nanT$_{PSL}$AR* and *nanEK nagA,* required for transport and catabolism of *N*-acetyl-neuraminic acid (Neu5Ac). A mutation of *nanR* abolished the extensive lag phase observed for the bacteria growing on Neu5Ac and increased transcription of *nanT$_P$* and *nanE,* suggesting that NanR is a transcriptional repressor of both *nan* operons. Intracellular accumulation of Neu5Ac was dependent on the carbon source, implying that the *nan* operons are also subject to catabolite repression. Hence, cAMP receptor protein (CRP) appeared to activate and repress transcription of *nanT$_{PSL}$AR* and *nanEK nagA,* respectively. Direct bindings of NanR and CRP to the *nanT$_P$-nanE* intergenic DNA were demonstrated by EMSA. Two adjacent NanR-binding sites centered at +44.5 and −10 and a CRP-binding site centered at −60.5 from the transcription start site of *nanT$_P$* were identified by DNase I protection assays. Mutagenesis approaches, *in vitro* transcription, and isothermal titration calorimetry experiments demonstrated that *N*-acetylmannosamine 6-phosphate specifically binds to NanR and functions as the inducer of the *nan* operons. The combined results propose a model in which NanR, CRP, and *N*-acetylmannosamine 6-phosphate cooperate for precise adjustment of the expression level of the *V. vulnificus nan* cluster.

When bacteria invade the human gut, adverse environmental changes, such as increased competition for the specific nutrients imposed by the host cells and endogenous bacterial flora, are encountered. As such, the ability to acquire nutrients under these adverse environments is often crucial for bacteria to survive and multiply in the intestine (1, 2). In the intestine, as the presence of free glucose is quite limited, enteropathogenic bacteria must be able to use alternative nutrients to be a successful pathogen (3, 4). Epithelial surfaces of the intestine exposed to bacteria are covered by a viscous mucous layer where bacteria primarily colonize (for a recent review see Ref. 5). The mucous layer contains mucins that are highly glycosylated polymorphic glycoproteins (6). Up to 85% of mucins are carbohydrates in dry weight (7), indicating that the mucin sugars are important carbon and energy sources to support the survival and growth of infecting enteropathogens.

Sialic acid represents a family of related nine-carbon sugar acids that are notably found at the distal end of carbohydrate side chains of mucins (for recent reviews see Refs. 8–10). The most abundant sialic acid is *N*-acetylneuraminic acid (Neu5Ac),[2] and therefore many intestinal commensal and pathogenic bacteria have evolved elaborate systems for the catabolic utilization of Neu5Ac. The bacteria employ different transporters to obtain Neu5Ac from the environments. For example, NanT of *Escherichia coli* belongs to the major facilitator superfamily, and SiaPQM of *Haemophilus influenzae* (or DctQPM of *Vibrio cholerae*) is a tripartite ATP-independent periplasmic transporter (9, 11). Regardless of the mode of Neu5Ac uptake, *N*-acetylneuraminate lyase (NanA) initiates the catabolism of Neu5Ac by cleaving it into pyruvate and *N*-acetylmannosamine (ManNAc) in most bacteria. ManNAc is ultimately converted into an intermediate of the central metabolism (fructose 6-phosphate) via the activities of various proteins, including NanK (*N*-acetylmannosamine kinase), NanE (*N*-acetylmannosamine-6-phosphate epimerase), and NagA (*N*-acetylglucosamine-6-phosphate deacetylase) as presented in Fig. 1*A* (8, 11).

[S] The on-line version of this article (available at http://www.jbc.org) contains supplemental Figs. S1–S3.

[1] To whom correspondence should be addressed: Dept. of Agricultural Biotechnology, Seoul National University, Seoul 151-921, South Korea. Tel.: 82-2-880-4857; Fax: 82-2-873-5095; E-mail: choish@snu.ac.kr.

[2] The abbreviations used are: Neu5Ac, *N*-acetylneuraminic acid; CRP, cAMP receptor protein; ManNAc-6P, *N*-acetylmannosamine 6-phosphate; ManNAc, *N*-acetylmannosamine; qRT-PCR, quantitative real time-PCR; RNAP, RNA polymerase; TSS, transcription start site; GlcNAc-6P, *N*-acetylglucosamine 6-phosphate; GlcN-6P, glucosamine 6-phosphate; ITC, isothermal titration calorimetry.

TABLE 1
Plasmids and bacterial strains used in this study

Strain or plasmid	Relevant characteristics[a]	Ref. or source
Bacterial strains		
V. vulnificus		
ATCC29307	Wild type *V. vulnificus*, virulent	Laboratory collection
DI0201	ATCC29307 with Δcrp	19
HG072	ATCC29307 with *nanA*::*nptI*, Km^r, Rif^r	13
BS0805	ATCC29307 with $\Delta nanR$::*nptI*, Km^r	This study
BS0902	BS0805 with Δcrp, Km^r	This study
BS1012	HG072 with $\Delta nanR$, Km^r, Rif^r	This study
BS1104	ATCC29307 with $\Delta nanE$	This study
E. coli		
SM10λpir	*thi thr leu tonA lacY supE recA*::RP4-2-Tc::Mu λ *pir*; Km^r; host for π-requiring plasmids; conjugal donor	18
BL21 (DE3)	F^-, *ompT*, *hsdS* (r_B^-, m_B^-), *gal* (DE3)	Laboratory collection
Plasmids		
pGEM-T easy	PCR product cloning vector; Ap^r	Promega
pBS0909	pGEM-T easy with intergenic region between *nanT$_P$* and *nanE*; Ap^r	This study
pDM4	Suicide vector; *oriR6K*; Cm^r	17
pBS1013	pDM4 with $\Delta nanR$; Cm^r	This study
pBS0907	pDM4 with Δcrp ; Cm^r	This study
pBS1102	pDM4 with $\Delta nanE$; Cm^r	This study
pHIS-Parallel1	Protein expression vector; Ap^r	22
pBS0820	pHIS-Parallel1 with *nanR*; Ap^r	This study
pHK0201	pRSET A with crp; Ap^r	23
pSH0505	pET28a with *V. vulnificus rpoD*, Km^r	25
pRLG770	General transcription vector; Ap^r	27
pBS0921	pRLG770 with P$_{nanE}$; Ap^r	This study

[a] The following abbreviations are used: Ap^r, ampicillin-resistant; Cm^r , chloramphenicol-resistant; Km^r, kanamycin-resistant; Rif^r, rifampicin-resistant.

Recently, to investigate the role of Neu5Ac catabolism in the pathogenesis of *Vibrio vulnificus*, a foodborne enteropathogen (12), a *nanA* mutant was constructed and used to evaluate phenotype changes. The *nanA* mutant was defective for intestinal colonization and significantly diminished in virulence in a mouse model (13). An independent study with *V. cholerae* demonstrated that the genes involved in the transport and catabolism of Neu5Ac are located in VPI-2 (*Vibrio* pathogenicity island 2), and the *nanA* mutant was also defective for colonization in the mouse intestine (14). These studies together suggested that the catabolic utilization of Neu5Ac is essential for the pathogenesis of the bacteria by ensuring growth and survival during infection (13, 14). Nevertheless, very little is known about the regulatory mechanism used by the bacteria to modulate the expression of the *Vibrio nan* clusters. Accordingly, in this study, the transcriptional units and promoters of the *V. vulnificus nan* genes were determined, and the roles of NanR, a putative transcription regulator, and CRP in the regulation of the *nan* genes were analyzed at the molecular level. In addition, ManNAc-6P, a Neu5Ac catabolic intermediate, was identified as an inducer that binds to NanR and alters its interaction with the *nan* promoter DNA.

EXPERIMENTAL PROCEDURES

Strains, Plasmids, Cloning of the Nan Intergenic Region, and Culture Media—The strains and plasmids used in this study are listed in Table 1. The 299-bp *nanT$_P$*-*nanE* intergenic DNA was amplified by PCR using primers NANT0903 and NANE0905 and cloned into pGEM-T easy (Promega) forming pBS0909. Unless noted otherwise, the *V. vulnificus* strains were grown in Luria-Bertani (LB) medium supplemented with 2.0% (w/v) NaCl (LBS) at 30 °C. When required, M9 (15), in which one of the carbon sources such as Neu5Ac (5 mM), xylose (10 mM), proline (10 mM), glycerol (0.2%, w/v), or glucose (0.2%, w/v) was supplemented, was used as a minimal medium. All chemicals were purchased from Sigma except ManNAc-6P, which was purchased from Carbosynth (Berkshire, UK).

Generation of nanR, nanE, nanR crp, and nanR nanA Mutants—*V. vulnificus nanR* on chromosome was amplified and inactivated *in vitro* by deletion of about two-thirds (550-bp of 837-bp) of the *nanR* ORF using the PCR-mediated linker-scanning mutation method as described elsewhere (16). Briefly, pairs of primers NANR0801F and NANR0801R (for amplification of the 5′ amplicon) or NANR0802F and NANR0802R (for amplification of the 3′ amplicon) were designed and used as listed in Table 2. The $\Delta nanR$, a 550-bp deleted *nanR*, was amplified by PCR using the mixture of both amplicons as the template and NANR0801F and NANR0802R as primers. Similar experimental procedures were adopted for amplification of the Δcrp and $\Delta nanE$ *in vitro*, except that primers CRP0901F, CRP0901R, CRP0902F, and CRP0902R (for 284-bp deleted *crp*) and NANE1001F, NANE1001R, NANE1002F, and NANE1002R (for 481-bp deleted *nanE*) were used, respectively, as indicated in Table 2. The resulting $\Delta nanR$, Δcrp, and $\Delta nanE$ were ligated with SphI-SalI digested pDM4 (17) to form pBS1013, pBS0907, and pBS1102, respectively (Table 1).

To generate the *nanR* mutant BS0805 by homologous recombination, *E. coli* SM10 λ *pir, tra* (containing pBS1013) (18), was used as a conjugal donor to *V. vulnificus* ATCC29307. Similarly, *E. coli* SM10 λ*pir, tra* containing either pBS1102, pBS0907, or pBS1013 was used as a conjugal donor in conjunction with one of the recipients ATCC29307, BS0805, and the *nanA* mutant HG0702 (13) to generate the *nanE* mutant BS1104, *nanR crp* mutant BS0902, and *nanR nanA* mutant BS1012 as indicated in Table 1. The conjugation and isolation of the transconjugants were conducted using the method described previously (19).

RNA Purification and Transcript Analysis—Total cellular RNA was isolated from the wild type and *nan* mutants grown to

TABLE 2
Oligonucleotides used in this study

Name	Oligonucleotide sequence, 5′ 3′[a]	Location[b]	Use
NANT0903	GTTGCAGCATTCGCAGAAAG	*nanT_P-nanE* intergenic region	Amplification of *nan* intergenic region, primer extension
NANE0905	CTCTTAGTATCGTATTGCGCTATGG	*nanT_P-nanE* intergenic region	Amplification of *nan* intergenic region, primer extension
NANR0801F	CTGCGCAACAAAAAGCCGATGTC	*nanR* flanking region	Mutant construction
NANR0801R	GCGGATCCGGTTTGGCTCAAATCAA	*nanR*	Mutant construction
NANR0802F	CCGGATCCGCAAGAAACAGCAGAAGTA	*nanR*	Mutant construction
NANR0802R	CGCTAACGCCATATGAGAGAGTAAAGAGG	*nanR* flanking region	Mutant construction
CRP0901F	TAGCTTGCAGCCTTAGTTAACAGC	*crp* flanking region	Mutant construction
CRP0901R	CTGGATCCTTGATTTAGGTAAGAAAGG	*crp*	Mutant construction
CRP0902F	AAGGATCCAGATCAAGATCACTCG	*crp*	Mutant construction
CRP0902R	CCCTGAAGGTTCGAGAATGC	*crp*-flanking region	Mutant construction
NANE1001F	AAATGTGATCGCGAACAGAAATTCGTC	*nanE*-flanking region	Mutant construction
NANE1001R	GACGACCTAAGCCAGTTATACGTTTTCAACGCCTTC	*nanE*	Mutant construction
NANE1002F	AACTGGCTTAGGTCGTCGTTTAATTCTGCAACACAAGC	*nanE*	Mutant construction
NANE1002R	GCCGCTTGAGCATCATTGAGC	*nanE*-flanking region	Mutant construction
NANR0809	CCATGGGTTCGCCGAAAAATTTATTAG	*nanR*	NanR overexpression
NANR0810	CTCGAGTTAATTTGCCATTAAAGGAATG	*nanR*	NanR overexpression
NANT_P_qRT_F	GCGTGCCGAATGCGAAACC	*nanT_P*	qRT-PCR
NANT_P_qRT_R	GATTCTCTTGCCCGTCAACTGC	*nanT_P*	qRT-PCR
NANE_qRT_F	TTCAGCCTGTTGTCGGTAGCC	*nanE*	qRT-PCR
NANE_qRT_R	CCTTCAATACGCAGTGCCTTAGC	*nanE*	qRT-PCR

[a] Regions of oligonucleotides not complementary to corresponding genes are underlined.
[b] Location indicate where the nucleotides were hybridized.

A_{600} of 0.6 with LBS and M9, supplemented with or without 5 mM Neu5Ac, using an RNeasy® mini kit (Qiagen) (20). For quantitative real time PCR (qRT-PCR), cDNA was synthesized with iScript[TM] cDNA synthesis kit (Bio-Rad), and real time PCR amplification of the cDNA was performed with the specific primer pairs for each *nan* gene (Table 2). Relative expression levels of the *nan* transcripts were calculated by using the 16 S rRNA expression level as the internal reference for normalization as described previously (21).

To determine the transcription start site of the $nanT_{PSL}AR$ operon, an end-labeled 20-base primer NANT0903 (Table 2) complementary to the coding region of $nanT_P$ was added to the RNA and then extended with SuperScript II RNase H⁻ reverse transcriptase (Invitrogen). The cDNA products were purified and resolved on a sequencing gel alongside sequencing ladders generated from pBS0909 (Table 1) with the same primer used for the primer extension. A transcription start site of the *nanEK nagA* operon was also determined using similar methods, except that primer NANE0905 was used in place of NANT0903 (Table 2). The primer extension products were visualized using a phosphorimage analyzer (BAS1500, Fuji Photo Film Co. Ltd., Tokyo, Japan).

Overexpression and Purification of V. vulnificus NanR and CRP—The *nanR* coding region was amplified by a PCR using the primers NANR0809 and NANR0810 (Table 2) and was then subcloned into a His₆ tagging expression vector, pHIS-Parallel1 (22), to result in pBS0820 (Table 1). The His-tagged NanR protein was then expressed in *E. coli* BL21 (*DE3*) and purified by affinity chromatography according to the manufacturer's protocol (Qiagen). Similarly, the expression and purification of the His-tagged CRP were carried out using pHK0201, carrying the *V. vulnificus crp* gene, as described elsewhere (23).

Electrophoretic Mobility Shift Assay (EMSA) and DNase I Protection Assay—The 299-bp $nanT_P$-*nanE* intergenic region, extending from residues −138 to +161 from the transcription start site of $nanT_{PSL}AR$ operon, was amplified by a PCR using ^{32}P-labeled NANT0903 and unlabeled NANE0905 as the primers (Table 2). The labeled 299-bp DNA (4 nM) fragment was incubated with varying concentrations of purified His-tagged NanR for 30 min at 37 °C in a 20-μl reaction mixture containing 1× binding buffer (24) and 1 μg of poly(dI-dC) (Sigma). The protein-DNA binding reactions with CRP were the same as those with NanR, except that the CRP binding buffer containing 1 mM cAMP was used as a 1× binding buffer (23). Electrophoretic analysis of the DNA·protein complexes have already been described (23).

The same 299-bp intergenic region was labeled by PCR amplification using a combination of ^{32}P-labeled and unlabeled primers, NANT0903 and NANE0905, and used for the DNase I protection assays. The binding of NanR or CRP to the labeled DNA was performed as described above and DNase I digestion of the DNA·protein complexes followed the procedures previously described (20). After precipitation with ethanol, the digested DNA products were resolved on a sequencing gel alongside sequencing ladders of pBS0909 generated using NANT0903 as the primer. The gels were visualized as described above for the primer extension analysis.

Purification of V. vulnificus RNA Polymerase (RNAP) Core Enzyme and RpoD—The *V. vulnificus* core RNAP was purified by an immunoaffinity chromatography using the polyol-responsive monoclonal antibody 8RB13 (NeoClone Biotechnology) as described previously (25, 26). The overexpression and purification of His-tagged RpoD were fulfilled using pSH0505, carrying the *V. vulnificus rpoD* gene, as described elsewhere (25). Purified RNAP core enzyme and RpoD proteins were dialyzed with the storage buffer (25), and equimolar amounts of the RNAP coreenzyme and RpoD were mixed on ice to generate the *V. vulnificus* RNAP holoenzyme before use.

In Vitro Transcription Assays—The 319-bp DNA fragment containing *nanEK nagA* promoter (P_{nanE}) region, isolated by digestion of pBS0909 with EcoRI, was recloned into pRLG770 that carries the *rrnB* terminator (27). The resulting plasmid pBS0921 (Table 1), as confirmed by DNA sequencing, was used as a template DNA to determine the effects of NanR and CRP
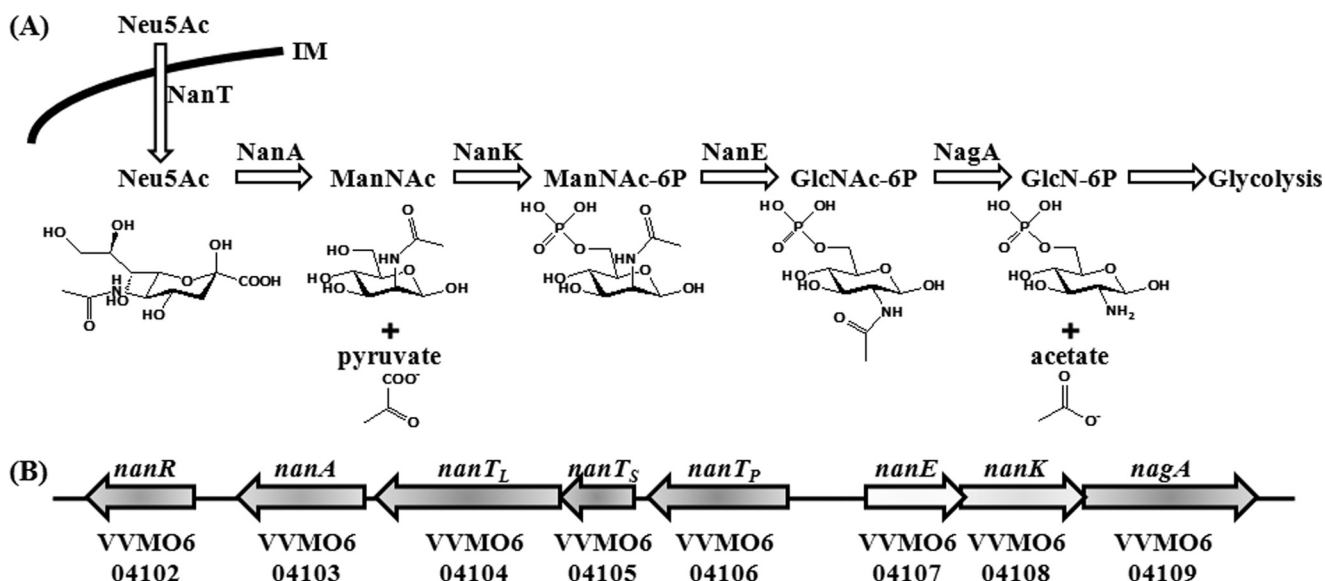
FIGURE 1. **Sialic acid catabolism and the *V. vulnificus nan* cluster.** *A,* schematic representation of the transport and catabolic pathway of sialic acid in bacteria is adopted from previously reported literature (8, 11). *B, arrows* represent the transcriptional directions and the coding regions of the *V. vulnificus nan* cluster. Gene names and locus tag numbers are based on the data base of the *V. vulnificus* MO6-24/O genome sequence (GenBank[TM] accession numbers CP002469 and CP002470; see Ref. 40). Proposed gene products are as follows: *nanR,* a putative transcriptional regulator; *nanA,* Neu5Ac lyase; *nanT_{PSL},* components of tripartite ATP-independent periplasmic type Neu5Ac transporter; *nanE, N*-acetylmannosamine-6-phosphate epimerase; *nanK, N*-acetylmannosamine kinase; *nagA, N*-acetylglucosamine-6-phosphate deacetylase.

on the transcription of P_{nanE} *in vitro*. Mixtures of the super-coiled pBS0921 DNA (0.4 nM) and NanR (or CRP with 1 mM cAMP), with or without Neu5Ac and its catabolic intermediates, at the concentrations indicated in the figure legends, were preincubated at 37 °C for 40 min in a reaction buffer described previously (28). The radiolabeled nucleotide (2 μCi of [$α$-^{32}P]UTP) and cold nucleotides (20 μM UTP and 400 μM each ATP, CTP, and GTP) were added to the mixture, and transcription was initiated by adding the *V. vulnificus* RNAP holoenzyme at the concentration of 0.25 nM. After incubation at 30 °C for 15 min, transcription was terminated by the addition of an equal volume of stop solution (25), electrophoresed on 7 M urea, 5.5% polyacrylamide gels, and processed as described for primer extension analysis.

Size-exclusion Chromatography and Isothermal Titration Calorimetry (ITC)—Purified NanR protein and ManNAc-6P were mixed in 1:100 molar ratio on ice for 2 h and subjected to size-exclusion chromatography using a Superdex 200 column (GE Healthcare) installed on an ÄKTA purifier FPLC system at room temperature with a flow rate of 0.35 ml/min. Apo-NanR was compared with the complex on the Superdex 200 column under the same condition. Aldolase (158 kDa) was used as a size reference protein. For ITC analyses, NanR protein, Neu5Ac, ManNAc-6P, and GlcN-6P were reconstituted in 0.5 mM DTT, 300 mM NaCl, and 50 mM Tris (pH 8.0). The calorimetric assays were performed as described previously (29). A 29 mM ligand solution in an injection syringe was titrated against 0.29 mM NanR in a reaction cell.

Data Analyses—Averages and standard errors of the mean (S.E.) were calculated from at least three independent trials. All data were analyzed by the Student's *t* test with the SAS program (SAS software; SAS Institute Inc., Cary, NC). Significance of differences between experimental groups was accepted at a *p* value of < 0.05.

RESULTS

Identification of the V. vulnificus nan Cluster—Many coding regions were identified immediately upstream and downstream of *nanA* from the *V. vulnificus* genome sequence (GenBank™ accession numbers AE016795 and AE016796). The postulated *V. vulnificus nan* cluster consists of the genes encoding a putative transcription regulator NanR, Neu5Ac transporters NanT_{PSL}, and proteins involved in catabolic degradation of Neu5Ac such as NanA, NanE, NanK, and NagA (Fig. 1*B*). The deduced amino acid sequences of the coding regions of the *V. vulnificus nan* cluster were 73–97% identical to those of the *nan* cluster from *V. cholera* (data not shown). The coding regions of the *V. vulnificus nan* cluster are organized in the same orientation as in the *V. cholerae nan* cluster (Fig. 1*B*, data not shown) (14). All of this information suggested that the products of the *nanT_{PSL}, nanA, nanE, nanK,* and *nagA* genes of the *V. vulnificus nan* cluster, are indeed involved in the transport and catabolic degradation of Neu5Ac as are the products of the *V. cholerae nan* cluster.

V. vulnificus nan Cluster Consists of Two Divergently Transcribed Operons—To analyze the expression pattern of the genes of the *V. vulnificus nan* cluster at the transcriptional level, the presence of transcripts of the intergenic regions of *nanR, nanA, nanT_{PSL}, nanE, nanK,* and *nagA* was examined using reverse transcription-PCR methods. The results revealed that *nanT_{PSL}, nanA,* and *nanR* were transcribed as a transcriptional unit, and another transcriptional unit consists of *nanE, nanK,* and *nagA* (data not shown). Therefore, it appeared that the *V. vulnificus nan* cluster consists of two operons, *nanT_{PSL}AR* and *nanEK nagA,* that are divergently transcribed as presented in Fig. 1*B*. The relative positions and transcriptional directions of the genes of the *V. vulnificus nan* cluster differ from those of the *E. coli* and *H. influenzae nan* clusters, which are relatively well
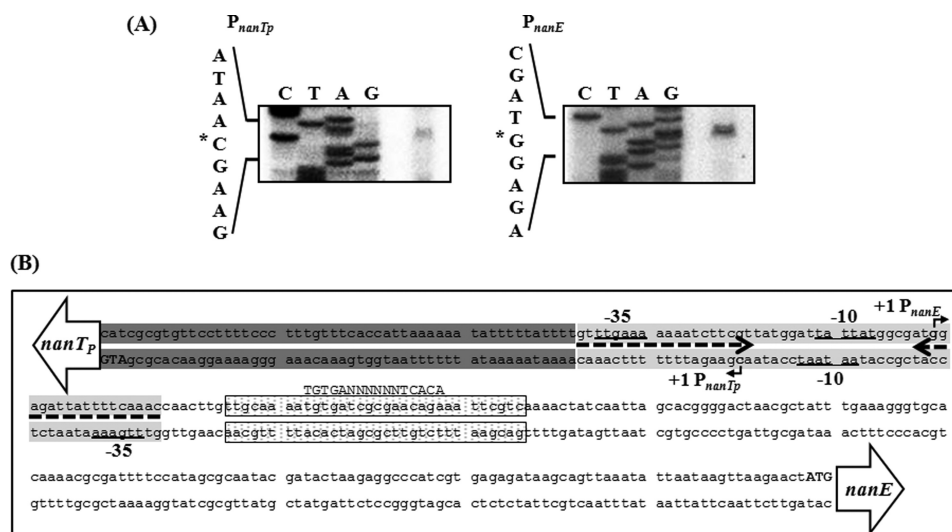
FIGURE 2. **Transcription start sites of P$_{nanTp}$ and P$_{nanE}$ and sequence analysis of the regulatory region of the *nan* operons.** *A,* TSSs, indicated by *asterisks*, were determined by primer extension of the RNA derived from the wild type (A_{600} 0.6) grown with LBS. *Lanes C, T, A,* and *G* represent the nucleotide sequencing ladders of pBS0909. *B,* TSS of P$_{nanTp}$ and P$_{nanE}$ are indicated by *bent arrows,* and the positions of their putative −10 and −35 regions are *underlined*. The NanR- and CRP-binding sequences determined later in this study (Fig. 5) are presented as a *shaded box* and a *dotted box*, respectively. The conserved nucleotide sequences for the binding of CRP are indicated *above* the *V. vulnificus* DNA sequence in *capital letters*. The translation initiation codons (ATG in *boldface*) and coding regions of *nanT$_P$* and *nanE* (*open arrows*) are also presented.

characterized at the molecular level (data not shown) (8, 30–32). These differences in genetic organization imply that the mechanisms for the regulation of the *V. vulnificus nan* cluster could be different from those of the *E. coli* and *H. influenzae nan* clusters.

Promoter Sequences for the nanT$_{PSL}$AR and nanEK nagA Operon Overlap—The transcription start sites of *nanT$_{PSL}$AR* and *nanEK nagA* were determined by primer extension analyses. A reverse transcript was identified from each primer extension of the RNA isolated from the wild type cells (Fig. 2A). The 5′ end of the *nanT$_{PSL}$AR* transcript is located 67 bp upstream of the translational initiation codon of *nanT$_P$* and subsequently designated +1. The putative promoter constituting this transcription start site was named P$_{nanTp}$ to represent the *nanT$_{PSL}$AR* promoter. The 5′ end of the *nanEK nagA* transcript is located 187 bp upstream of the start codon of *nanE* and is designated +1 of P$_{nanE}$ (the *nanEK nagA* promoter). Despite several attempts, no other transcription start sites were identified by primer extension analyses using different sets of primers hybridizing to the coding region of the *nan* cluster (data not shown). The sequences for −10 and −35 regions of both P$_{nanTp}$ and P$_{nanE}$ were assigned on the basis of similarity to consensus sequences of the *E. coli* σ^{70} promoter (Fig. 2B). It was noteworthy that the sequences for P$_{nanTp}$ and P$_{nanE}$ are partially overlapped, and four nucleotides of the −10 boxes are shared by each other (Fig. 2B).

Construction of the nanR Mutants and Their Growth in Presence of Neu5Ac—To explore the role of NanR in the regulation of the *V. vulnificus nan* cluster, the *nanR* isogenic mutants were constructed by allelic exchanges (Table 1). Double crossovers, in which each wild type *nanR* on the chromosome was replaced with the Δ*nanR* allele, were confirmed using previously described methods (data not shown) (19). The growth of the *nanR* mutant BS0805 and its parental wild type was not significantly different in LBS (data not shown). However, the *nanR*

mutant showed a significantly reduced lag phase ($p < 0.05$) compared with that of the wild type when cultured in M9 with Neu5Ac as a sole carbon source (supplemental Fig. S1A). Hence, disruption of *nanR* markedly increased growth on Neu5Ac, indicating that NanR functions as a repressor for the *nan* operons encoding proteins required for the transport and catabolism of Neu5Ac.

It has been known that the intracellularly accumulated Neu5Ac is toxic and inhibits the growth of *E. coli* (33). When Neu5Ac was added to the *nanR* mutant growing on glucose, growth of the mutant was not substantially inhibited, reflecting that Neu5Ac was not able to accumulate to the level of toxicity (supplemental Fig. S1B). This result can be explained if the genes for the catabolic degradation as well as transport of Neu5Ac were induced simultaneously by the *nanR* mutation, which provides further evidence for NanR acting as a repressor of both *nan* operons. Consistent with this assumption, growth of the *nanR nanA* double mutant, in which the NanA is inactivated and thereby catabolic degradation of Neu5Ac is blocked, was substantially inhibited by Neu5Ac (supplemental Fig. S1B). Growth inhibition by Neu5Ac was also dependent on the carbon source; larger inhibition zones by Neu5Ac were observed for the *nanR nanA* mutant growing on glycerol rather than glucose (supplemental Fig. S1B). This observation suggested that Neu5Ac accumulation was accelerated by growth on glycerol and that the expression of the *nan* genes, or at least *nanT$_{PSL}$*, is subject to catabolite repression.

NanR Negatively Regulates Both the P$_{nanTp}$ and P$_{nanE}$ Activities—To examine the effect of NanR on P$_{nanTp}$ and P$_{nanE}$, the transcripts of *nanT$_P$* and *nanE*, the first genes of the *nanT$_{PSL}$AR* and *nanEK nagA* operons, respectively, were quantitated in the same amount of total RNA isolated from the wild type and *nanR* mutant. Compared with the wild type, the *nanR* mutant revealed an almost 60-fold increase in *nanT$_P$* expression and a 15-fold increase in *nanE* expression (Fig. 3, *A* and *B*).
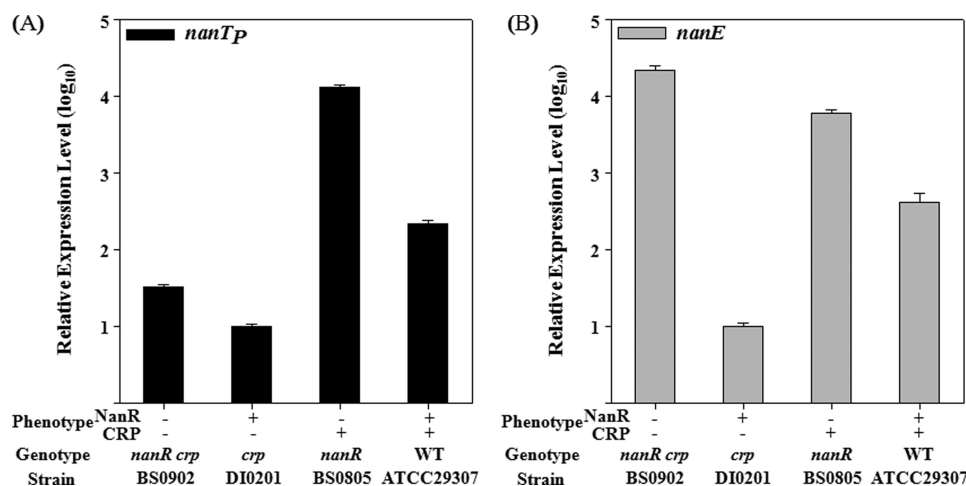
FIGURE 3. **Expression of *nanT_P* and *nanE* in *V. vulnificus* with different genetic backgrounds.** Cultures of the wild type, the *nanR*, *crp*, and *nanR crp* double mutants as indicated were grown with LBS, and samples removed at A_{600} of 0.6 were used to isolate total cellular RNA. The relative levels of *nanT_P* (*A*) and *nanE* (*B*) expression were determined by qRT-PCR analyses and normalized to the 16 S rRNA expression level as presented the expression level of the *crp* mutants as 1 in $\log_{10}$. *Error bars* represent the S.E.

These results confirmed that both *nan* operons are under negative control of NanR and supported our previous observation that growth on Neu5Ac was accelerated by the mutation of *nanR*.

CRP Regulates the P_{nanTp} and P_{nanE} Activities Differentially—To investigate the role of CRP in the regulation of P_{nanTp}, *nanT_P* expression of the wild type and *crp* mutant was compared (Fig. 3*A*). Inactivation of *crp* resulted in reduction of *nanT_P* expression, and the residual *nanT_P* expression level of the *crp* mutant corresponded to only one-twentieth that of the wild type. This suggested that the CRP functions as an activator for P_{nanTp}. This activation of P_{nanTp} by CRP is consistent with our previous assumption that more Neu5Ac accumulates in the *nanR nanA* mutant growing on glycerol than on glucose (supplemental Fig. S1*B*).

Notably, *nanE* expression of the *crp* mutant decreased to only one-fortieth that of the wild type (Fig. 3*B*), and thus CRP appeared to elevate the P_{nanE} activity. Despite this, CRP possibly stimulates *nanE* expression either directly by activating P_{nanE} or indirectly by alleviating the NanR-mediated repression of P_{nanE}. To distinguish these possibilities, the *nanR crp* double mutant was constructed, and *nanE* expression was quantitated (Table 1 and Fig. 3*B*). An additional inactivation of *crp* in the *nanR* mutant led to a 3.6-fold increase in *nanE* expression, indicating that CRP negatively regulates P_{nanE} in the absence of NanR (Fig. 3*B*). Consequently, these results suggested that CRP activates P_{nanTp} and represses P_{nanE} and thereby regulates the *nanT_{PSL}AR* and the *nanEK nagA* operons differentially.

NanR and CRP Function Cooperatively Rather Than Sequentially to Regulate the nan Operons—The mutagenesis approaches implicated that both NanR and CRP played important roles in the regulation of the *nan* cluster. However, different mechanisms were still possible for the regulation of P_{nanTp} by NanR and CRP. For example, CRP indirectly up-regulated the P_{nanTp} activity by inhibiting *nanR* expression and thereby relieving the promoter from the negative control of NanR. To test this possibility, expression levels of *nanT_P* of the *nanR* mutant and *nanR crp* double mutant were compared (Fig. 3*A*).

An additional inactivation of *crp* in the *nanR* mutant resulted in about a 400-fold decrease in *nanT_P* expression, indicating that the CRP activates P_{nanTp} in the absence of NanR (Fig. 3*A*). Similarly, an additional mutation of *nanR* in the *crp* mutant led to a 3-fold increase in *nanT_P* expression, indicating that NanR represses P_{nanTp} in the absence of CRP (Fig. 3*A*). Consequently, it seems most likely that CRP and NanR regulate P_{nanTp} cooperatively rather than sequentially in a regulatory cascade. However, it is also noteworthy that an additional mutation of *nanR* in the *crp* mutant led to an almost 2000-fold increase in *nanE* expression in the absence of CRP, whereas mutation of *nanR* resulted in only a 15-fold increase in the presence of CRP (Fig. 3*B*). This observation suggested that the repression of P_{nanE} by NanR is affected by CRP.

NanR and CRP Specifically Bind to the P_{nanTp} and P_{nanE} Regulatory Region—The 299-bp DNA fragment encompassing the *nanT_P-nanE* intergenic region was incubated with increasing amounts of NanR and then subjected to electrophoresis. As seen in Fig. 4*A*, the addition of NanR resulted in a concentration-dependent ladder of two retarded bands, indicating that at least two binding sites with different affinities for NanR are present within the *nanT_P-nanE* intergenic region. The binding of NanR was also specific, because assays were performed in the presence of 1 μg of poly(dI-dC) as a nonspecific competitor. In a second EMSA, the same but unlabeled 299-bp DNA fragment was used as a self-competitor to confirm the specific binding of NanR. The unlabeled 299-bp DNA competed for the binding of NanR in a dose-dependent manner (Fig. 4*A*, *lanes 5–7*), confirming that NanR binds specifically to the DNA. In similar DNA-binding assays, CRP also displayed specific binding to the *nanT_P-nanE* intergenic region (Fig. 4*B*). These results indicated that NanR and CRP were able to bind to their operator within the *nanT_P-nanE* intergenic region by themselves in the absence of the other in an independent manner. When both proteins were included in the binding reaction, they bound simultaneously to their operator and presented a slower moving band of DNA bound with both of the proteins as demonstrated by an EMSA in Fig. 4*C*.
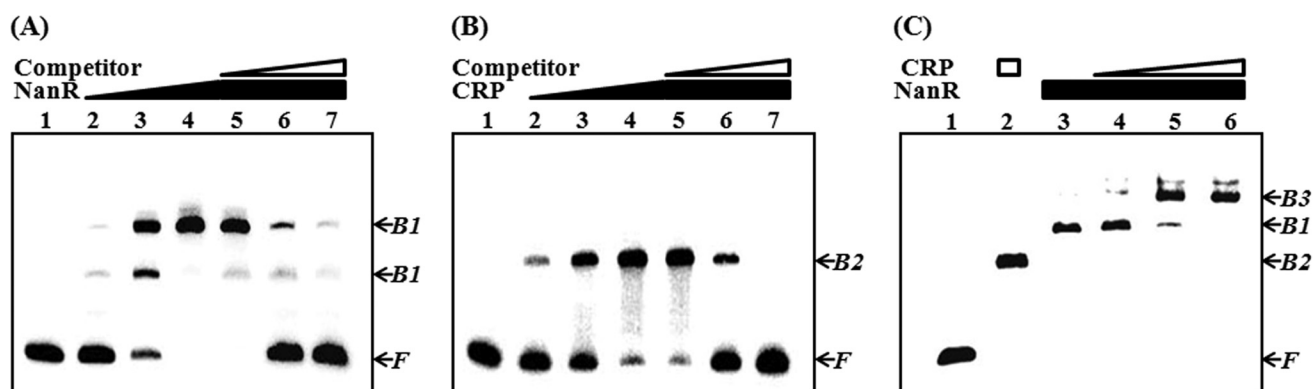
FIGURE 4. **EMSA for binding of NanR and CRP to the *nanT$_P$-nanE* intergenic region.** A 299-bp DNA fragment of the *nanT$_P$-nanE* intergenic region was radioactively labeled and used as a probe for DNA. The radiolabeled fragments (4 nM) were mixed with increasing amounts (0, 10, 50, and 100 nM in the *lanes 1–4*, respectively) of NanR (*A*) or CRP (*B*) and then resolved on a 5% polyacrylamide gel. For competition analysis, the same but unlabeled 299-bp DNA fragment was used as a self-competitor DNA. The labeled DNA probe was incubated with the self-competitor DNA (at 12.5, 37.5, and 75 nM, from *lanes 5 to 7*, respectively) prior to the addition of 200 nM NanR (*A*) or CRP (*B*). *C*, mixtures of 100 nM NanR and increasing amounts of CRP were added to the labeled DNA probe as indicated. *Lane 1*, no protein; *lane 2*, 200 nM CRP; *lanes 3–6* (in the presence of 100 nM NanR), 0, 10, 50, 100 nM CRP, respectively. The positions of the unbound fragments (*F*), and the fragments retarded by NanR (*B1*), CRP (*B2*), or mixture of NanR and CRP (*B3*) are indicated by *arrows*.

Identification of Binding Sites for NanR and CRP Using DNase I Protection Analysis—When the sequences for the binding of NanR to the intergenic region of *nanT$_P$-nanE* were mapped with NanR up to 100 nM, the NanR footprint extended from -37 to $+18$ relative to the transcription start site (TSS) of P$_{nanTp}$ (Figs. 5*A* and 2*B*). When increasing the NanR, another region extending from $+70$ to $+19$ was protected from DNase I digestion (Figs. 5*A* and 2*B*). This sequential protection with increasing NanR was consistent with the previous observation that at least two binding sites with different affinities for NanR are present in the intergenic region (Fig. 4*A*). The regions extending from -37 to $+18$ (centered at -10) and from $+70$ to $+19$ (centered at $+44.5$) were named NANRBI and NANRBII, to represent the NanR-binding sites I and II, respectively. Inspection of the sequences extending from -37 to $+18$ revealed a 19-bp (GTTTGAAAAAAATCTTCGT) inverted repeat. In contrast, the sequences from NANRBII, to which NanR bound with lower affinity, does not carry the 19-bp inverted repeat (Figs. 5*A* and 2*B*), indicating that the inverted repeat is important for NanR binding with higher affinity. Because the sequences of NANRBI overlap with the sequences of -10 and -35 regions of P$_{nanE}$ as well as P$_{nanTp}$, bound NanR would be expected to prevent RNAP binding. This result supported our previous observation that NanR functions as a repressor for both promoters.

Similar DNase I protection assays were performed with CRP, and the DNase I footprinting revealed a clear protection pattern in the *nanT$_P$-nanE* intergenic region extending from -45 to -76 (centered at -60.5) relative to TSS of P$_{nanTp}$ (Fig. 5*B*). The sequences of the protected region scored 87.5% similar to a consensus sequence for CRP binding (the TGTGAN[6–8] TCACA, see Ref. 34). This position for CRP binding indicated that the P$_{nanTp}$ is a class I CRP-dependent promoter. For class I CRP-dependent promoters, CRP-binding sites are centered at near integral turns of the helix (*i.e.* $n \times 10.5$ bp) from TSS (35). These observations confirmed that CRP activates P$_{nanTp}$ directly, by binding to the upstream region of P$_{nanTp}$. However, the CRP-binding site is located downstream of P$_{nanE}$ and centered at $+40.5$ from the TSS of P$_{nanE}$. Therefore, from the
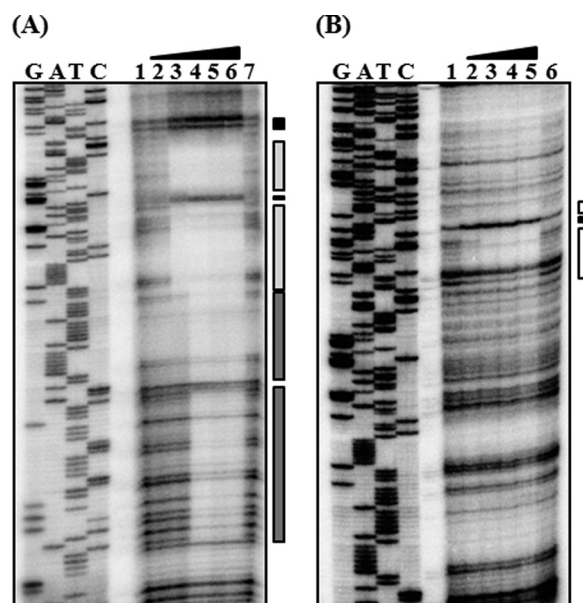

FIGURE 5. **Identification of binding sites for NanR and CRP.** DNase I protection analysis of NanR (*A*) and CRP (*B*) binding to the intergenic region of *nan* operons. The ^{32}P-labeled 299-bp DNA fragments were incubated with increasing amounts of NanR or CRP and then digested with DNase I. *A*, *lanes 1* and *7*, no NanR added; *lanes 2–6*, NanR at 50, 100, 200, 400, and 800 nM, respectively. *B*, *lanes 1* and *6*, no CRP added; *lanes 2–5*, CRP at 100, 200, 400, and 800 nM, respectively, with 1 mM cAMP. *Lanes G, A, T,* and *C* represent the nucleotide sequencing ladders of pBS0909. The regions protected by NanR are indicated by *light* (NANRBI) and *dark* (NANRBII) *shaded boxes* (*A*), and the regions protected by CRP are indicated by *open boxes* (*B*). The nucleotides showing enhanced cleavage are indicated by *black boxes*.

standpoint of P$_{nanE}$, CRP bound to the binding site could hinder RNAP movement and thereby repress its activity. This idea supported our earlier observation that CRP negatively regulates P$_{nanE}$. Taken together, these results demonstrated that NanR and CRP control P$_{nanTp}$ and P$_{nanE}$ directly by binding to their respective operators independently.

Neu5Ac Induction of the nan Operons Increased by the Mutation of nanE—Exogenous addition of Neu5Ac resulted in induction of the *E. coli nanATEK* operon and displaced NanR from its operator *in vitro* as demonstrated by EMSA (30). As shown in Fig. 6, addition of Neu5Ac to *V. vulnificus* growing on

M9 with xylose and proline as sources of nutrient led to the induction of $nanT_P$ and $nanE$ by 48- and 35-fold, respectively. However, it was still possible that intermediates of the Neu5Ac catabolic pathway, rather than Neu5Ac, influence induction of the *nan* genes. To test this possibility, the effects of either *nanA* or *nanE* mutation on the Neu5Ac-dependent induction of the $nanT_P$ and $nanE$ were explored by the qRT-PCR analyses (Fig. 6). Neither $nanT_P$ nor $nanE$ was induced by Neu5Ac in the *nanA* mutant, and their expression levels were indistinguishable from the wild type levels obtained in the absence of Neu5Ac (Fig. 6). Because Neu5Ac should accumulate in the *nanA* mutant, this result indicated that Neu5Ac is not the inducer for $nanT_P$ and $nanE$. In contrast, expression levels of both genes were significantly greater ($p < 0.05$) in the *nanE* mutant than in the wild type (Fig. 6). The enzyme converting ManNAc-6P to *N*-acetylglucosamine-6-phosphate (GlcNAc-6P) is lacking, and thus ManNAc or ManNAc-6P would be accumulated in the *nanE* mutant. These results implied that ManNAc or ManNAc-6P, the intermediates of Neu5Ac catabolism, could be an inducer for the induction of both *nan* operons.

ManNAc-6P Specifically Alleviates the Repression by NanR— It was apparent that one of the Neu5Ac catabolic intermediates, rather than Neu5Ac, alleviates the NanR-mediated repression of the *nan* operons. To identify the inducer, effects of ManNAc and ManNAc-6P on the activity of P_{nanE} were analyzed in the presence of purified NanR protein by *in vitro* transcription assays (Fig. 7). Consistent with our previous result, the P_{nanE} activity was completely repressed in the presence of 100 nM NanR protein, and addition of Neu5Ac was not able to alleviate the NanR repression. In contrast, the addition of ManNAc-6P was able to relieve the NanR-mediated repression and induce the P_{nanE} activity, indicating that ManNAc-6P is the inducer displacing the NanR from its operator. It is noteworthy that the addition of other catabolic intermediates of Neu5Ac, such as ManNAc, GlcNAc-6P, and glucosamine 6-phosphate (GlcN-6P), was unable to induce the P_{nanE} activity *in vitro* at all (Fig. 7).

ManNAc-6P Interacts Directly with NanR— Size-exclusion chromatography showed that NanR exists mainly as a hexameric species in solution. The same oligomerization pattern was observed for the NanR·ManNAc-6P complex with a slight increase in molecular weight, suggesting that there may be a conformational change of NanR with the ligand (Fig. 8A). To further evaluate whether ManNAc-6P interacts directly with the NanR protein, ITC experiments were performed. The ITC results revealed that ManNAc-6P binds to NanR with a model of sequential binding to the hexameric NanR molecules with different binding affinities. The ligand binding affinities for the first to the sixth NanR molecules resulted in dissociation constants (K_d) ranging from 1.39 μM to 2.3 mM (Fig. 8, *B* and *C*). However, no interactions were observed between the NanR and other sugars such as Neu5Ac (supplemental Fig. S2A) and GlcN-6P (supplemental Fig. S2B). These results suggest that ManNAc-6P is a specific inducer to relieve NanR-mediated repression of the *nan* operons.
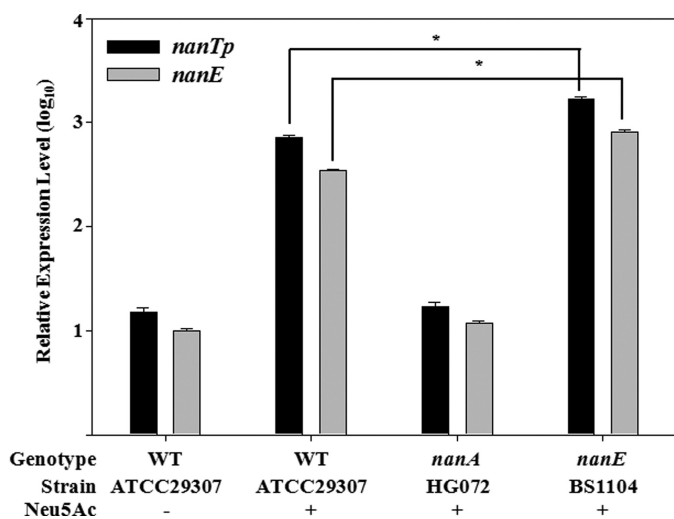
FIGURE 6. **Effects of Neu5Ac on the $nanT_P$ and $nanE$ expression of *V. vulnificus* with different genetic backgrounds.** The wild type, the *nanA*, and *nanE* mutants were grown with M9 medium supplemented with 10 mM D-xylose and 10 mM L-proline in the presence or absence of Neu5Ac as indicated, and samples removed at A_{600} of 0.6 were used to isolate total cellular RNA. The relative levels of the $nanT_P$ and $nanE$ transcripts were determined by qRT-PCR analyses and normalized to the 16 S rRNA expression level as presented the $nanE$ transcript level of the wild type in the absence of Neu5Ac as 1 in $\log_{10}$. *Error bars* represent the S.E.
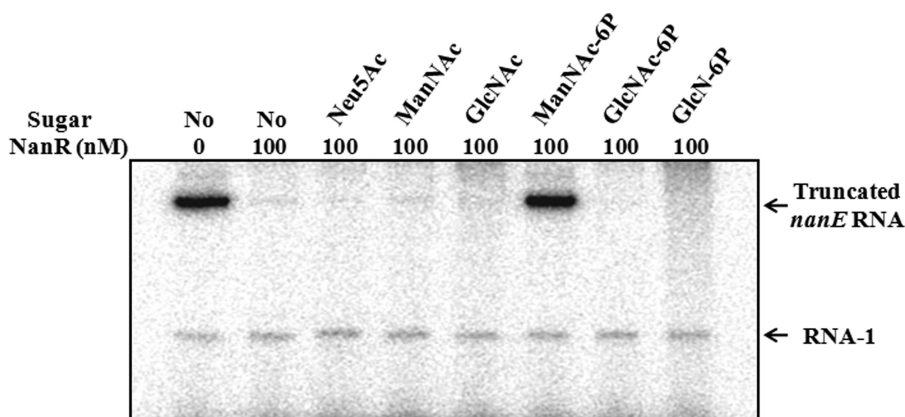
FIGURE 7. **Effects of Neu5Ac and its catabolic intermediates on the NanR repression of P_{nanE} *in vitro*.** Supercoiled plasmid pBS0921 containing the P_{nanE} was used as a template DNA and transcribed *in vitro* in the presence of 100 nM NanR. Either Neu5Ac or one of its catabolic intermediates (1 mM) such as ManNAc, GlcNAc, ManNAc-6P, GlcNAc-6P, and GlcN-6P were added to the supercoiled template DNA as indicated. The 370-base P_{nanE}-specific transcripts and vector-derived control transcripts RNA-1 are indicated.
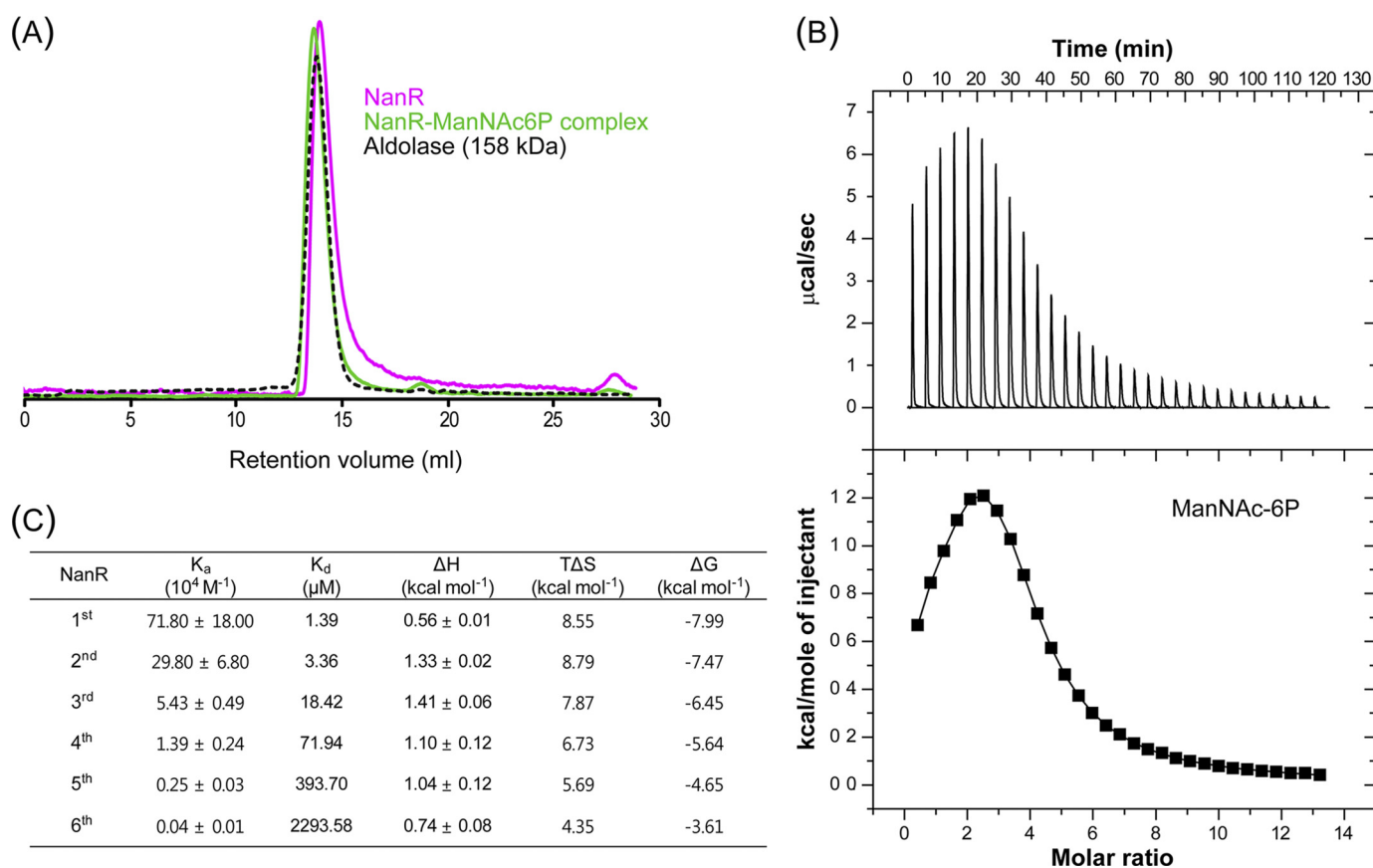
NanR	K_a $(10^4 M^{-1})$	K_d (μM)	ΔH $(kcal\ mol^{-1})$	$T\Delta S$ $(kcal\ mol^{-1})$	ΔG $(kcal\ mol^{-1})$
1st	71.80 ± 18.00	1.39	0.56 ± 0.01	8.55	-7.99
2nd	29.80 ± 6.80	3.36	1.33 ± 0.02	8.79	-7.47
3rd	5.43 ± 0.49	18.42	1.41 ± 0.06	7.87	-6.45
4th	1.39 ± 0.24	71.94	1.10 ± 0.12	6.73	-5.64
5th	0.25 ± 0.03	393.70	1.04 ± 0.12	5.69	-4.65
6th	0.04 ± 0.01	2293.58	0.74 ± 0.08	4.35	-3.61

FIGURE 8. **ManNAc-6P binds specifically to NanR.** *A,* NanR and ManNAc-6P complex exists as hexameric form in solution. Apo-NanR and complex are indicated by *magenta* and *green*, respectively. Aldolase (158 kDa) shown by the *black dashed line* was used as a size marker. *B,* typical isothermal titration calorimetric measurement of the interaction between the NanR protein and ManNAc-6P. The raw data are displayed in the *upper panel*, and integration plot of the data is displayed in the *lower panel*. *C,* thermodynamic parameters of the interaction between the NanR protein and ManNAc-6P. The representative ITC results were calculated using the best fit model (sequential binding sites model), and the heat data of ligand into the reaction buffer was subtracted from the reaction heat data between protein and ligand.

DISCUSSION

The diversity in the gene order and in the structure of *nan* clusters may be a common feature inherited among bacteria as proposed by Vimr *et al.* (8). Phylogenetic analyses indicated that the genes within the *nan* clusters show independent evolutionary histories (11). *E. coli* NanR and *H. influenzae* SiaR, major regulators of the *nan* clusters, belong to different families of transcription regulators. *E. coli* NanR and *H. influenzae* SiaR are members of the FadR/GntR and RpiR family, respectively (31). *V. vulnificus* NanR carries a highly conserved phospho-sugar-binding (SIS) domain of the RpiR family (36), and thereby possibly falls into the RpiR family. However, the amino acid sequences of *V. vulnificus* NanR show low levels of identity (28%) to those of SiaR (data not shown). From this overall lack of similarity among NanR (SiaR) proteins, it is not surprising that the sialic acid catabolism of *V. vulnificus* is regulated through its own regulatory system that is different from that for *E. coli* and *H. influenzae*.

NanR and CRP negatively and positively regulate *E. coli nan* genes, where *nanA* and *nanT* encoding a sialic acid transporter and *nanEK* are transcribed in the same directions. Neu5Ac is an inducer and displaces NanR from its operators to induce the *nan* genes (30). In *H. influenzae*, CRP activates only the *siaPT* operon (encoding transporters), which is transcribed diver-

gently from the *nanEK siaR nagAB* operon in the presence of cAMP (31, 32). In the absence of Neu5Ac, SiaR binds to the *siaP-nanE* intergenic region to repress both *siaPT* and *nanEK siaR nagAB* operons. It was surprising that SiaR changed from repressor to activator in the presence of GlcN-6P, a catabolic intermediate of Neu5Ac. The SiaR·GlcN-6P complex was presumed to bind to the *siaPT-nanE* intergenic region, with even greater affinity, to activate the *siaPT* and *nan* operons, and thus GlcN-6P is a coactivator rather than an inducer (32).

In this study, *V. vulnificus* NanR binds to the $nanT_P$-*nanE* intergenic region to repress both $nanT_{PSL}AR$ and *nanEK nagA* operons in the absence of Neu5Ac. This negative feedback regulation of *nanR* could prevent overexpression of NanR and thus allow a basal level expression of transporters ($NanT_{PSL}$), which is necessary for the initial uptake of Neu5Ac when the bacteria encounter Neu5Ac (Fig. 3 and supplemental Fig. S1). Increased induction of $nanT_P$ and *nanE* in the *nanE* mutant proposed that ManNAc-6P, rather than Neu5Ac, is an inducer for the *nan* cluster (Fig. 6). ManNAc-6P weakened binding of NanR to the $nanT_P$-*nanE* intergenic DNA *in vitro*, whereas Neu5Ac and other catabolic intermediates of Neu5Ac had no effect on NanR binding to the DNA as determined by an EMSA (data not shown). Consistent with this, *in vitro* transcription assay revealed that only ManNAc-6P, not Neu5Ac and other Neu5Ac

catabolic intermediates, was able to relieve the NanR-mediated repression of P_{nanE} (Fig. 7). Furthermore, among the tested amino sugars, only ManNAc-6P specifically interacts with NanR (Fig. 8, *B* and *C*, and [supplemental Fig. S2](#)). These combined results confirmed that ManNAc-6P binds to NanR and induces the *nan* operons of *V. vulnificus*.

Many catabolic activities are typically regulated by the presence of the substrate acting as an inducer. *V. vulnificus* likely uses ManNAc-6P as an inducer because transported Neu5Ac can be toxic to cells unless it is utilized rapidly. If Neu5Ac is used as an inducer, transport of Neu5Ac into cells would occur even in the presence of a preferred sugar (*e.g.* glucose) in addition to Neu5Ac, which would result in toxic accumulation of the nonpreferred Neu5Ac, as opposed to catabolic degradation. In contrast, by using ManNAc-6P as an inducer, induction of the *nan* operons and high level Neu5Ac uptake would be initiated only when the preferred sugar is completely consumed, and catabolism of Neu5Ac has indeed progressed to yield a sufficient amount of ManNAc-6P.

It is noted that CRP regulates P_{nanTp} and P_{nanE} differentially (Fig. 3). The CRP-binding site is centered at −60.5 bp upstream from the transcription start site of $nanT_P$, and this distance is typical for a class I CRP activation (Figs. 2*B* and Fig. 5*B*) (37). However, this CRP-binding site is centered +40.5 bp from the TSS of *nanE*, where the CRP represses P_{nanE}, presumably by acting a roadblock for RNAP (38, 39). An *in vitro* transcription assay demonstrated that addition of CRP led to the reduction of the transcription from P_{nanE}, confirming the CRP-dependent repression of P_{nanE} ([supplemental Fig. S3](#)). For growth on Neu5Ac as a sole carbon source, a complete displacement of NanR from the operator is necessary for full induction of P_{nanTp} and a strong expression of $NanT_{PSL}$. Although P_{nanE} is also induced by the lack of NanR on the operator, the induction would be rather moderate as a result of the CRP-dependent repression. The moderate (or adequate) expression of P_{nanE} could keep the catabolic degradation rate of ManNAc-6P from outpacing the uptake rate of Neu5Ac, ensuring that a sufficient amount of the inducer is available in cells to maintain the full induction of P_{nanTp}.

Interestingly, the P_{nanE} activity in the wild type was higher than that of the *crp* mutant (Fig. 3*B*). This increased activity of P_{nanE} by the presence of functional CRP might be the result of the position of the P_{nanTp} −35 and −10 regions that entirely overlap the NanR-binding site required for repression of P_{nanE} as well as P_{nanTp} by NanR (Fig. 2*B*). As such, RNAP recruited by the CRP bound for activation of P_{nanTp} could hinder the binding of NanR to its operator and eliminate the NanR-mediated repression of P_{nanE}. The resulting inductive effect would be pronounced enough to mask the CRP-dependent roadblock effect and thereby CRP appeared to increase the P_{nanE} activity.

Fig. 9 summarizes our current understanding of the regulation of *V. vulnificus nan* cluster. When the bacteria are starved, RNAP recruited by CRP for activation of P_{nanTp} could interfere with NanR binding to its operator and result in low but significant activity of P_{nanE} as well as P_{nanTp}. When a preferred sugar(s) is available, NanR alone, not CRP, could bind strongly to its operator and repress both *nan* operons tightly. When only Neu5Ac is available, ManNAc-6P displaces NanR from its
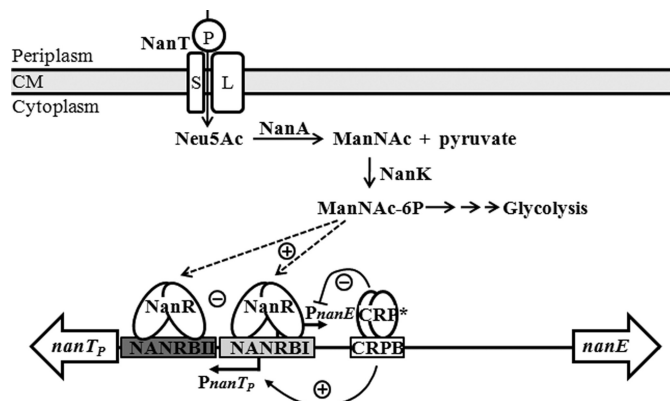
FIGURE 9. **Proposed model for regulation of the *V. vulnificus nan* cluster by NanR, CRP, and ManNAc-6P.** When the bacteria grow on Neu5Ac as a sole carbon source, a strong expression of P_{nanTp} is necessary, which is possibly obtained by the class I activation by CRP in addition to ManNAc-6P-mediated displacement of NanR bound to its operator (NANRBI and MANRBII) overlapping the −35 and −10 region of P_{nanTp}. P_{nanE} is also induced by the lack of NanR on the operator; the induction would be rather moderate as a result of the CRP binding to its operator (*CRPB*) and thus acting as a roadblock for RNAP. The moderate expression of P_{nanE} maintains ManNAc-6P sufficient for growth on Neu5Ac, which is probably encountered in the intestine. −, negative regulation; +, positive regulation; *CM*, cytoplasmic membrane.

operator, and additional activation by CRP renders P_{nanTp} the strength of full induction. CRP also represses the P_{nanE} as a roadblock to maintain a sufficient level of ManNAc-6P in cells, which is necessary for the full induction of P_{nanTp} and efficient growth in this growth condition, presumably encountered in the host intestine.

REFERENCES

1. Chang, D. E., Smalley, D. J., Tucker, D. L., Leatham, M. P., Norris, W. E., Stevenson, S. J., Anderson, A. B., Grissom, J. E., Laux, D. C., Cohen, P. S., and Conway, T. (2004) *Proc. Natl. Acad. Sci. U.S.A.* **101,** 7427–7432
2. Brown, S. A., Palmer, K. L., and Whiteley, M. (2008) *Nat. Rev. Microbiol.* **6,** 657–666
3. Hooper, L. V., Midtvedt, T., and Gordon, J. I. (2002) *Annu. Rev. Nutr.* **22,** 283–307
4. Lång, H., Jonson, G., Holmgren, J., and Palva, E. T. (1994) *Infect. Immun.* **62,** 4781–4788
5. McGuckin, M. A., Lindén, S. K., Sutton, P., and Florin, T. H. (2011) *Nat. Rev. Microbiol.* **9,** 265–278
6. Larsson, J. M., Karlsson, H., Sjövall, H., and Hansson, G. C. (2009) *Glycobiology* **19,** 756–766
7. Wiggins, R., Hicks, S. J., Soothill, P. W., Millar, M. R., and Corfield, A. P. (2001) *Sex Transm. Infect.* **77,** 402–408
8. Vimr, E. R., Kalivoda, K. A., Deszo, E. L., and Steenbergen S. M. (2004) *Microbiol. Mol. Biol. Rev.* **68,** 132–153
9. Severi, E., Hood, D. W., and Thomas, G. H. (2007) *Microbiology* **153,** 2817–2822
10. Angata, T., and Varki, A. (2002) *Chem. Rev.* **102,** 439–469
11. Almagro-Moreno, S., and Boyd, E. F. (2009) *BMC Evol. Biol.* **9,** 118
12. Jones, M. K., and Oliver, J. D. (2009) *Infect. Immun.* **77,** 1723–1733
13. Jeong, H. G., Oh, M. H., Kim, B. S., Lee, M. Y., Han, H. J., and Choi, S. H. (2009) *Infect. Immun.* **77,** 3209–3217
14. Almagro-Moreno, S., and Boyd, E. F. (2009) *Infect. Immun.* **77,** 3807–3816
15. Sambrook, J., and Russell D. W. (2001) *Molecular Cloning: A Laboratory Manual,* 3rd Ed., Section A2.2, Cold Spring Harbor Laboratory Press,

Cold Spring Harbor, NY

16. Lee, J. H., Kim, M. W., Kim, B. S., Kim, S. M., Lee, B. C., Kim, T. S., and Choi, S. H. (2007) *J. Microbiol.* **45,** 146–152

17. Milton, D. L., O'Toole, R., Horstedt, P., and Wolf-Watz, H. (1996) *J. Bacteriol.* **178,** 1310–1319

18. Miller, V. L., and Mekalanos, J. J. (1988) *J. Bacteriol.* **170,** 2575–2583

19. Jeong, H. S., Lee, M. H., Lee, K. H., Park, S. J., and Choi, S. H. (2003) *J. Biol. Chem.* **278,** 45072–45081

20. Lee, J. H., and Choi, S. H. (2006) *Mol. Microbiol.* **60,** 513–524

21. Oh, M. H., Lee, S. M., Lee, D. H., and Choi, S. H. (2009) *Infect. Immun.* **77,** 1208–1215

22. Sheffield, P., Garrard, S., and Derewenda, Z. (1999) *Protein Expr. Purif.* **15,** 34–39

23. Choi, H. K., Park, N. Y., Kim, D. I., Chung, H. J., Ryu, S., and Choi, S. H. (2002) *J. Biol. Chem.* **277,** 47292–47299

24. Rhee, J. E., Jeong, H. G., Lee, J. H., and Choi, S. H. (2006) *J. Bacteriol.* **188,** 6490–6497

25. Lee, H. J., Park, S. J., Choi, S. H., and Lee, K. H. (2008) *J. Biol. Chem.* **283,** 30438–30450

26. Bergendahl, V., Thompson, N. E., Foley, K. M., Olson, B. M., and Burgess, R. R. (2003) *Protein Expr. Purif.* **31,** 155–160

27. Ross, W., Thompson, J. F., Newlands, J. T., and Gourse, R. L. (1990) *EMBO J.* **9,** 3733–3742

28. Newlands, J. T., Gaal, T., Mecsas, J., and Gourse, R. L. (1993) *J. Bacteriol.* **175,** 661–668

29. Kim, Y., Kim, B. S., Park, Y. J., Choi, W. C., Hwang, J., Kang, B. S., Oh, T. K., Choi, S. H., and Kim, M. H. (2010) *J. Biol. Chem.* **285,** 14020–14030

30. Kalivoda, K. A., Steenbergen, S. M., Vimr, E. R., and Plumbridge, J. (2003) *J. Bacteriol.* **185,** 4806–4815

31. Johnston, J. W., Zaleski, A., Allen, S., Mootz, J. M., Armbruster, D., Gibson, B. W., Apicella, M. A., and Munson, R. S., Jr. (2007) *Mol. Microbiol.* **66,** 26–39

32. Johnston, J. W., Shamsulddin, H., Miller, A. F., and Apicella, M. A. (2010) *BMC Microbiol.* **10,** 240

33. Vimr, E. R., and Troy, F. A. (1985) *J. Bacteriol.* **164,** 845–853

34. Botsford, J. L., and Harman, J. G. (1992) *Microbiol. Rev.* **56,** 100–122

35. Ebright, R. H. (1993) *Mol. Microbiol.* **8,** 797–802

36. Bateman, A. (1999) *Trends Biochem. Sci.* **24,** 94–95

37. Barnard, A., Wolfe, A., and Busby, S. (2004) *Curr. Opin. Microbiol.* **7,** 102–108

38. Santangelo, T. J., and Artsimovitch, I. (2011) *Nat. Rev. Microbiol.* **9,** 319–329

39. Toulmé, F., Mosrin-Huaman, C., Artsimovitch, I., and Rahmouni, A. R. (2005) *J. Mol. Biol.* **351,** 39–51

40. Park, J. H., Cho, Y. J., Chun, J., Seok, Y. J., Lee, J. K., Kim, K. S., Lee, K. H., Park, S. J., and Choi, S. H. (2011) *J. Bacteriol.* **193,** 2062–2063